LAWRENCE
LIVERMORE
NATIONAL
LABORATORY

LLNL-PROC-420432

Ultra-fast photoluminescence as a diagnostic for laser damage initiation

T. A. Laurence, J. D. Bude, N. Shen, P. E. Miller, W. A. Steele, G. Guss, J. J. Adams, L. L. Wong, M. D. Feit, T. I. Suratwala

November 19, 2009

Boulder Damage Symposium
Boulder, CO, United States
September 21, 2009 through September 23, 2009

Disclaimer

Ultra-fast photoluminescence as a diagnostic for laser damage initiation

Ted A. Laurence, Jeff D. Bude, Nan Shen, Philip E. Miller, William A. Steele, Gabe Guss, John J. Adams, Lana L. Wong, Michael D. Feit, Tayyab I. Suratwala, Lawrence Livermore National Laboratory

Abstract

Using high-sensitivity confocal time-resolved photoluminescence (CTP) techniques, we report an ultra-fast photoluminescence (40ps–5ns) from impurity-free surface flaws on fused silica, including polished, indented or fractured surfaces of fused silica, and from laser-heated evaporation pits. This fast photoluminescence (PL) is not associated with slower point defect PL in silica which has characteristic decay times longer than 5ns. Fast PL is excited by the single photon absorption of sub-band gap light, and is especially bright in fractures. Regions which exhibit fast PL are strongly absorptive well below the band gap, as evidenced by a propensity to damage with 3.5eV ns-scale laser pulses, making CTP a powerful non-destructive diagnostic for laser damage in silica. The use of CTP to provide insights into the nature of damage precursors and to help develop and evaluate new damage mitigation strategies will be presented.

Introduction

There are a number of flaws in fused silica surfaces which are linked to initiation of laser damage in fused silica. The creation of surface flaws by scratching or indentation, previous laser-damage, or the redeposition of silica vapor surrounding CO_2 laser-heated evaporation pits creates laser damage precursors – regions susceptible to surface damage from ns-scale high fluence laser pulses.[1] These damaged regions are susceptible to exponential growth upon exposure to further laser pulses. Such regions with low laser-induced damage thresholds limit the performance of high fluence laser systems, such as laser-based inertial confinement fusion systems considered for nuclear energy production.[2, 3]

The nature of the laser damage precursors has proven elusive for many years.[4, 5] Damage precursors absorb sub-band-gap light, raising the temperature around the precursor high enough (in excess of the boiling point[6-8]) to result in explosive ejection of material from the surface. Typical laser fluences for silica surface damage range from 1 J/cm^2 (for poor surfaces) to 40 J/cm^2 (for excellent surfaces) for a 3 ns, 3.5 eV laser pulse. This absorption occurs over a broad range of photon energies as low as 1eV, much lower than the 9eV silica band-gap; for example, the damage threshold for silica surface flaws can be below 10 J/cm^2 at 2.3eV (532nm).[9] The bulk damage threshold for a 3 ns, 3.5 eV laser pulse is over 160 J/cm^2. In this case, three-photon absorption creates free carriers, which then absorb further laser energy to reach the boiling point. For the intensities involved in laser damage of surface flaws, multi-photon ionization is extremely unlikely.[7] Multi-photon ionization occurs typically for I>100 GW/cm^2, whereas intensities for a 5 J/cm^2, 3ns laser pulse is <2 GW/cm^2. Three photon absorption decreases as the cube of intensity so that, for these intensities, there is negligible three-photon absorption.

Most models assume that precursors must reach the boiling point in order to cause physical damage. We assume that the laser damage fluence, ϕ_{TH}, must be enough to deposit at least enough laser energy to increase the silica temperature to the boiling point of ~ 2500K. A minimum absorption coefficient, $\alpha_{min,}$ can be estimated by assuming no heat lost to diffusion (providing a lower bound); using a heat capacity of $C_p \approx 2.6$ J/cm^3 – K, and $\phi_{TH} = 5$ J/cm^2 (0.5N indent), $\alpha_{min} = \Delta T\, C_p / \phi_{TH} \sim 1200$ cm^{-1}. This absorptivity is surprisingly high, approaching the absorptivity

of metals. Contamination by metallic impurities certainly leads to damage – the damage threshold for 12nm gold nano-particles imbedded near the silica surface has been measured to be 4.6J/cm^2 for 355nm, 0.5ns pulses.[8] However, impurity-free surface flaws like the static indentations studied here often damage at thresholds below those observed for the imbedded gold nanoparticles.

We introduced the use of high-sensitivity Confocal Time-resolved Photoluminescence (CTP) imaging, often used in single molecule biophysics, to probe the light-matter interactions in near surface regions of optical materials [10] (Fig. 1). CTP enables high resolution three-dimensional PL imaging (2-3μm along optical path, submicron in transverse directions) in dielectrics. A 3.1 eV pulsed laser (400 nm, LDH-P-C-405B, Picoquant) is focused using a high numerical aperture objective (UMPLFL 100X, NA=0.95, Olympus) onto a fused silica sample. Scattering and luminescence excited by the laser are collected by the same objective and focused onto a confocal pinhole (100μm; excluding out-of-focus luminescence). Two spectral channels (550-610 nm, >665 nm) and a scattering channel are monitored by avalanche photodiodes (Micro Photon Devices PDM 50CT). Each detected photon is time-stamped with its absolute arrival time (50 ns resolution) and its arrival time relative to the laser pulse (measuring PL lifetime with 150-300ps resolution) using a time-to-digital converter (PicoHarp 300, Picoquant). The sample is scanned in 3 dimensions using a piezo scanner (Nano-LP-200, MadCityLabs). Data acquisition and analysis are performed using custom software written in LabVIEW.

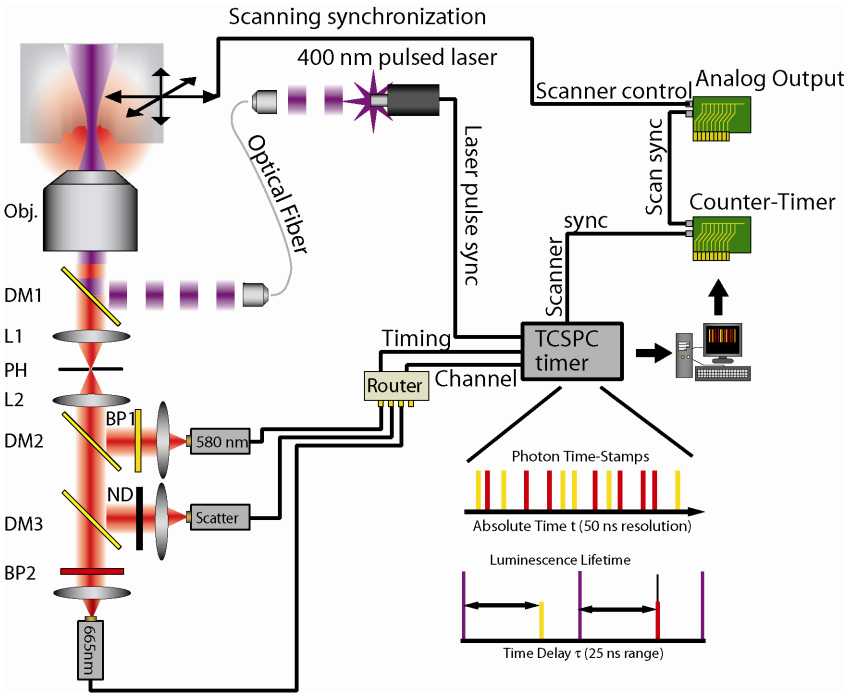

Figure 1: Experimental setup for confocal time-resolved photoluminescence measurements. We have adapted high sensitivity confocal fluorescence lifetime microscopy for characterizing luminescence near fused silica surfaces with a wide variety of surface conditions. A pulsed laser (LDH-P-C-405B, Picoquant, Berlin) is focused using a high numerical aperture objective (UMPLFL 100X, NA=0.95, Olympus) onto a fused silica sample. Scattering and luminescence excited by the laser are collected by the same objective and focused onto a confocal pinhole (100μm). Two spectral channels (BP1: 550-610 nm; BP2: >665 nm) and a scattering channel are monitored by avalanche photodiodes (Micro Photon Devices PDM 50CT). Each detected photon is time-stamped with its absolute arrival time (100 ns resolution) and its arrival time relative to the laser pulse (150 ps for the 400 nm laser to 500 ps for the 635 nm laserincluding laser and

APD response) using a time-to-digital converter (PicoHarp 300, Picoquant, Berlin). The sample is scanned in 3 dimensions using a piezo scanner (Nano-LP-200, MadCityLabs, Madison, Wisconsin), and the scanner is controlled using custom software written in LabVIEW (National Instruments, Austin, Texas) to control three analog axes (PCI-6731 And PCI-6052E, National Instruments). The experiment is synchronized with a counter-timer board (PCI-6602, National Instruments). Using a luminosity standard (Model 63355, Oriel-Newport, Stratford, Connecticut), the detection efficiency of the optical system was measured as approximately 20% in the yellow range. Including effects of collection angles of the objective, we estimate an overall detection efficiency of nearly 5%.

The use of CTP for studying laser damage precursors is motivated by the fact that optically active transitions involved in absorption must also luminesce, even if weakly. The observed PL lifetime τ_{PL} results from a competition between the rates of radiative pathways k_{PL} and non-radiative pathways k_{NR}: $\tau_{PL}=1/(k_{PL}+k_{NR})$. Known silica point defects[11, 12] have PL lifetimes ranging from 2ns to milliseconds; only the non-bridging oxygen hole center with τ_{PL} =13μs and the oxygen deficiency center II with τ_{PL} =10ms are excited at or below 3.5eV.[13] For 3.5eV photons, raising the temperature of silica from 300K to 2500K requires the aborption (no reemission) of 10^{22} photons/cm^3. By comparison, the density of Si-O bonds in silica is ~$5\cdot10^{22}$ cm^{-3}. The defects mentioned above decay on time scales much longer than the 3ns laser pulse. In order to raise the temperature of surface flaws to the silica boiling point within a 3ns laser pulse, we expect much shorter-lived electronic excitations with τ_{PL} <3ns.

Electrons excited into continuum electronic states, such as those in a metal, decay very rapidly through non-radiative, single phonon emission, so that the perceived PL lifetimes, $\tau_{PL} \approx 1/k_{NR}$, are very short, and PL emission very weak.[14-16] The strong absorption (>1000cm^{-1}) of silica surface flaws suggests a high density of electronic states typical of metals. Consequently, we look for PL which behaves more like a metal than point defects. Although a true continuum of electronic states in silica surface flaws is not expected due to the wide band gap, a high density of absorbing electronic states would lead to PL considerably faster than point defects (<<1ns). An additional possible strong absorption mechanism would involve excited state absorption of point defects [17]. In this case, we would find fast PL associated with the presence of point defects. Below, we compare the presence of slow (point defect) PL and fast PL, and find a fast PL uncorrelated with the presence of slow Pl, but correlated with laser damage susceptibility. CTP has the sensitivity and resolution necessary to detect such small regions of absorbing material emitting weak, fast PL, as well as the ability to determine the lifetime of the luminescence transitions.

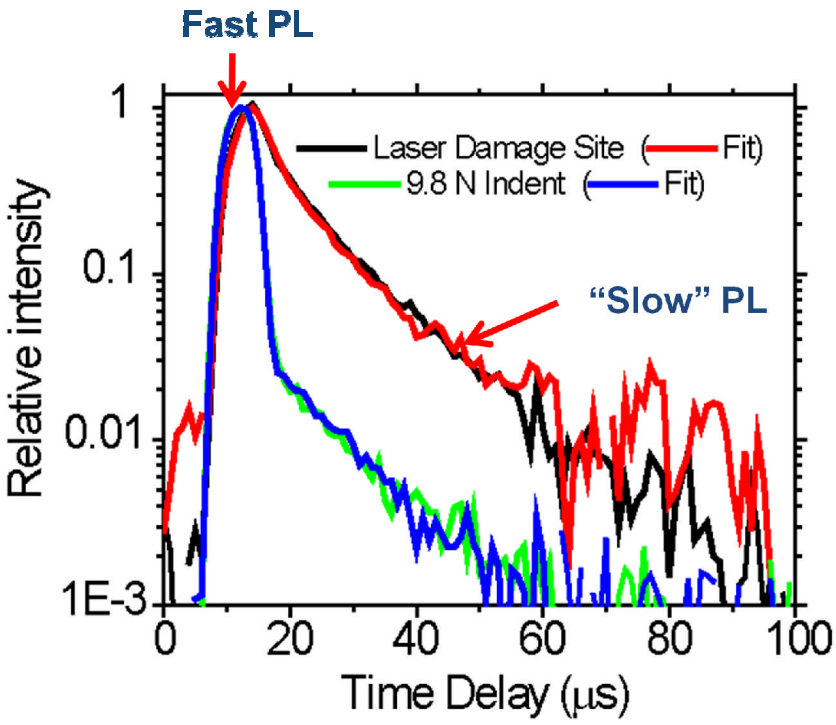

Figure 2: CTP measurements of "slow" decay of non-bridging oxygen hole center (NBOHC) using a 633 nm laser switched on for 10 microseconds every 100 microsecond period. Black: NBOHC observed in laser damage site. Red: Fit using exponential convolved with measured instrument response. Green: Fast PL (short time) and slow PL observed in 9.8 Vicker's indentation. Blue: Fit to exponential convolved with instrument response.

CTP sees both the point defects known to exist in bulk silica and on its surface and a previously unidentified complex fast PL response having a wide distribution of PL lifetimes. Previous spectroscopic studies of stress-induced point defects in silica[18] and of laser damaged silica surfaces[19-21] have revealed several intrinsic point defects found in bulk silica[13]. Under 633nm excitation, we observe the well known non-bridging oxygen-hole center (NBOHC, the oxygen part of a broken Si-O bond) in laser damage sites, identified by its spectrum and its 13μs PL lifetime (black line Fig. 2)[13]. The Gaussian fit of the spectral line matches previous observations (1.92eV mean, 0.2eV half-width). However, under 400nm excitation, the laser damage site exhibited a wide, featureless. For a Vicker's indentation in silica, the NBOHC spectrum is not visible upon excitation at 633nm, only a much wider emission is seen. The characteristic NBOHC lifetime is clearly detected in the indentation (green line, Fig. 2), but the signal is dominated by much faster decay components. Weaker fast components are also seen in the damage site (black line, Fig. 2). In fact, a similar PL behavior is seen for all the features measured here, at both 400nm and 633nm excitation.

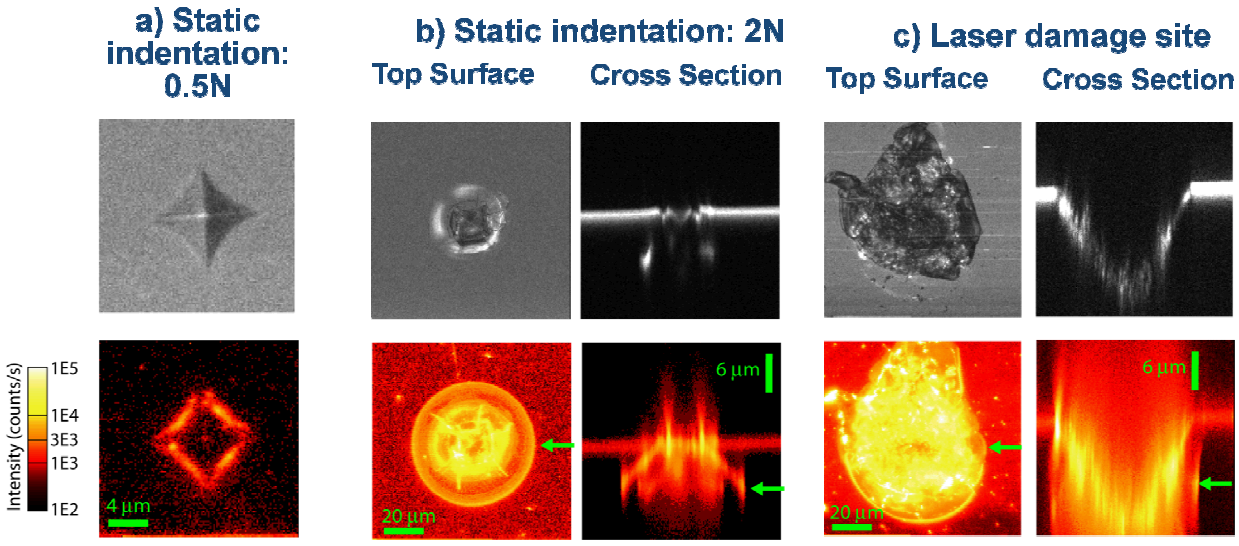

Figure 3: CTP images of scattering (top) and photoluminescence (bottom) from damage-prone silica surface flaws. **(a).** 0.5N silica indentation. **(b).** 2N silica indentation (surface view left). Plane through surface along green arrow on right. **(c)**. Laser damage site (surface view left). Plane through surface along green arrow on right.

We report CTP measurements of a variety of silica surface flaws (Fig. 3) and measure their laser damage threshold with 3ns, 355nm laser pulses. We identify a fast PL that correlates strongly to regions with a propensity for laser damage. This PL is not from any known defects in silica.[11, 12] The flaws measured here were produced on optical grade Corning 7980 fused silica samples: laser damage sites (Fig. 3c) were produced by focused 3ns Gaussian laser pulses at 355nm with a $1/e^2$ diameter of about 100µm; static indentations were created with a Vicker's indenter with various loads (2N, Fig. 3b; 0.5N, Fig. 3a). Surface features were also created through local heating using a focused 10.6µm CO_2 laser (not shown); the surface was heated to about 2200K, creating a 200µm wide, 5µm deep, damage-resistant evaporation pit surrounded by a ring of damage-prone redeposited material formed by condensation of silica vapor.

Figure 3 shows time integrated PL images along with the corresponding optical scattering images of the surface flaws studied here. All show PL with a variety of strong lifetime components from 40ps-5ns (e.g. red line in Fig. 4), hereafter referred to as "fast PL". By modulating the laser intensity with an electro-optic modulator, we found in all cases that the PL was linear in excitation intensity, and hence involves only single-photon processes. Polished silica surfaces show very weak fast PL. In contrast to the fast PL, all known silica point defects have PL lifetimes which are $\geq$ 2ns;[13, 22] in many of the flaws, we have identified the non-bridging oxygen hole center by its lifetime (green line) and spectrum. The PL from silver nano-particles (black line) is faster than our time resolution (~150ps) and is used as an instrument response function, convolved with the exponential decays, for lifetime fitting. Figure 4b shows that the fast PL lies between the extremes of the PL from metallic nanoparticles and the known point defects of fused silica.

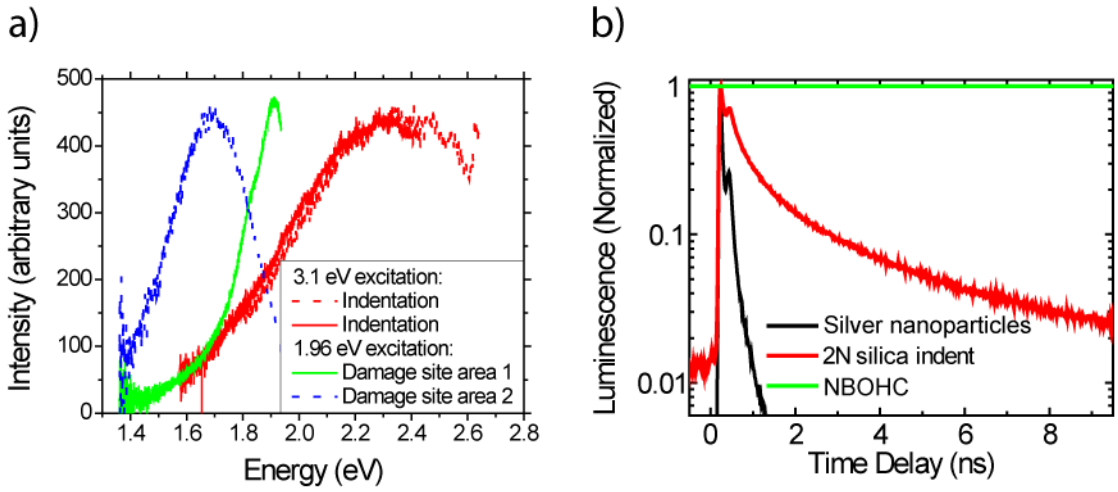

Figure 4: a) Luminescence spectra of damage sites and statics indentations on fused silica surfaces. Compare the wide, relatively featureless spectra shown in red (at 3.1 eV excitation) and blue (at 1.96 eV excitation) to the spectrum of the NBOHC found in certain areas of the laser damage site (green). b) High time resolution (~100 ps) photoluminescence lifetime decays of damage-prone silica surface flaws (integrated over entire flaw; red), silver nanoparticles (black), and the non-bridging oxygen hole center (NBOHC) (calculated from fit; green)

Fast PL in silica originates within several hundred nm of the surface and is strongly enhanced near fracture surfaces. Large fracture networks can form around 2N indentations, including cone fractures which extend up to 10μm below the surface;[23] strong fast PL clearly follows these fractures, and weak fast PL is associated with the polished surface (Fig. 3). The deep fractures were not in contact with the indenter, hence fast PL cannot be caused by contamination from the indenter. Although a 0.5N indentation forms a layer of densified silica beneath it,[23] the fast PL is only observed along the edges of the indentation (Fig. 3a).

By extracting the total strengths of each lifetime component over an image, we can separate the fast PL components which correlate to damage propensity from the slow PL components which do not. Four lifetime components from 0.04ns to 5ns are required to fit the fast PL measured here; we interpret this to mean there is a distribution of lifetime components, rather than four specific values. For image extraction, we fit the total number of photons for each lifetime component, with fixed lifetimes of 0.04ns, 0.2ns, 1ns, and 5ns, and a constant component for PL >25ns. In the CO_2 laser-heated pits, two rings of luminescence are observed (Fig. 5). The bright, inner ring of the CO_2 laser pit is dominated by long lifetimes. The outer ring of redeposited material has stronger fast components, and is where laser damage occurs upon exposure to a high fluence 3ns laser pulse (green arrow). Fast PL dominates the luminescence from indentations, so that images separating fast PL components from slow PL components are nearly identical to the total PL images. Central regions of laser damage sites contain slow PL (Fig. 6), matching the regions where the non-bridging oxygen hole center is observed with a 633nm laser.

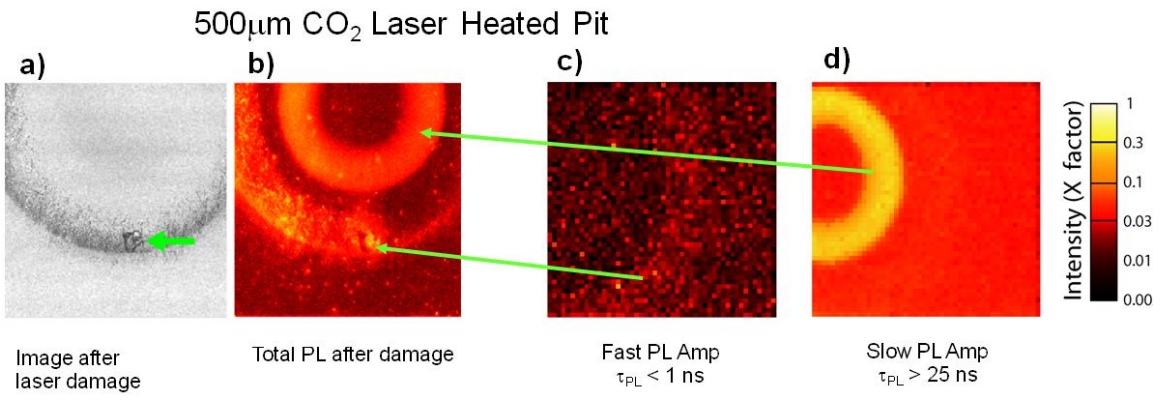

Figure 5: Extracted "fast" and "slow" PL of CO_2 laser heated pit. a) Scattering image of apit after laser damage. B) Total Pl of pit in (a) showing two successive rings of PL. c) PL with fast lifetimes is associated with regions undergoing laser damage. d) PL with slow lifetimes is not associated with laser damage.

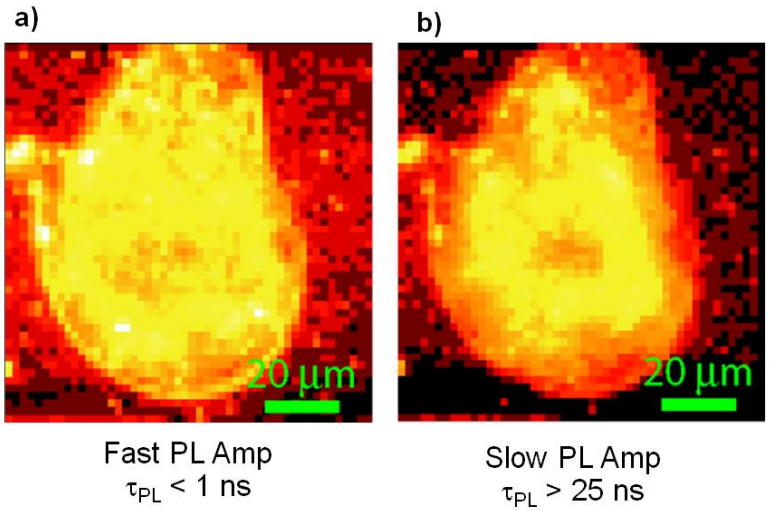

Figure 6: Extracted "fast" and "slow" PL of laser damage site. a) Image of strength of fast components (< 1ns decay times). b) Image of strength of slow components (>25ns decay times).

Fast PL is directly linked to areas that exhibit strong absorption leading to laser damage. After CTP imaging the surface features above, we measured the laser damage threshold with focused 3ns Gaussian laser pulses at 355nm with a $1/e^2$ diameter of about 100μm (Fig. 7). The 0.5 N indentations damage at the edges, precisely where the fast PL is observed. By performing a short etch (5 minute buffered oxide etch-BOE), we remove about 200nm of material, and also remove the PL; annealing of 0.5N indentations for 48 hrs at 750C removes the luminescence even more dramatically . Both processes significantly increase the damage threshold (Fig. 8). The CO_2 laser heated sites damage on the redeposit where the fast PL is found, but not where the bright, slow PL is found. Figure 8 shows the correlation between maximum fast (<1ns) PL and laser damage thresholds for the features measured here. This correlation holds for the surface treatments measured here; for our measurement conditions, the discrimination sensitivity is greater for damage thresholds below 20 J/cm^2. Also shown is the slow (>>25ns) point-defect-like PL extracted from the CTP for these surface regions; slow PL shows no direct correlation to damage. Note particularly

that the 0.5N indent shows very little, and often no detectable, slow PL, but has a damage threshold significantly lower than the surface threshold. Also, the CO_2 laser mitigation spot shows a strong slow PL signal, but has a relatively high damage threshold. Understanding the physics which drives this unexpected fast PL will lead to a deeper understanding of the electronic structure and optical properties of dielectric surface regions.

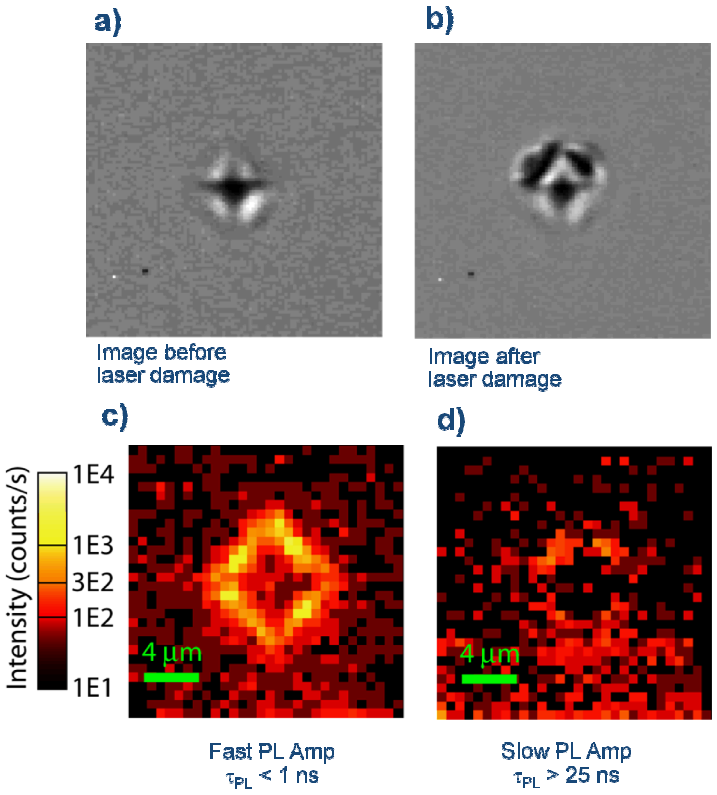

Figure 7: Images of 0.5 N indentation before (a) and after (b) laser damage. c) The damage occurs precisely where there are strong fast lifetime components (<1ns). d) Slow (>25 ns) components are weak or absent in 0.5 N indentations.

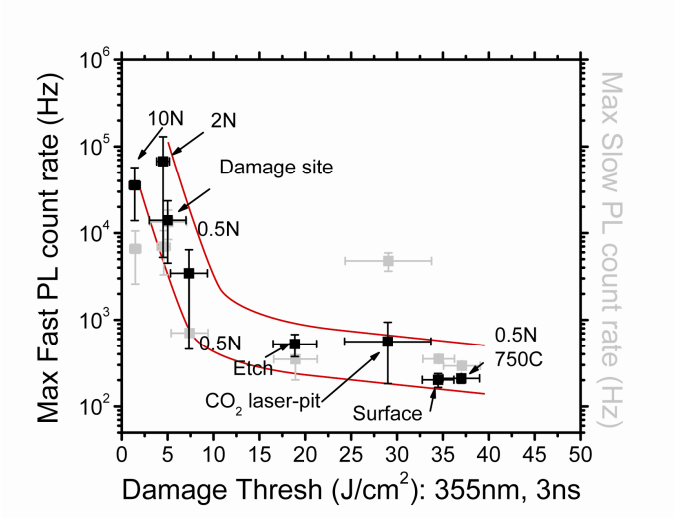

Figure 8: Maximum fast PL count rate vs. laser damage thresholds for the silica surface flaws with mean and standard deviation shown in both axes (black). Indentation loads from 0.5N to 10N and BOE etch or 750C anneal are noted on graph. Maximum slow PL count rate shown in gray. Red lines are a guide for the eye.

This work performed under the auspices of the U.S. Department of Energy by Lawrence Livermore National Laboratory under Contract DE-AC52-07NA27344. This work was supported by the laboratory directed research and development (LDRD) program at LLNL.

References

1. Stuart, B.C., et al., *Nanosecond-to-femtosecond laser-induced breakdown in dielectrics.* Physical Review B, 1996. **53**(4): p. 1749-1761.
2. Nuckolls, J., et al., *Laser Compression of Matter to Super-High Densities: Thermonuclear (CTR) Applications.* Nature, 1972. **239**(5368): p. 139.
3. Lindl, J., *Development Of The Indirect-Drive Approach To Inertial Confinement Fusion And The Target Physics Basis For Ignition And Gain.* Physics Of Plasmas, 1995. **2**(11): p. 3933-4024.
4. Glass, A.J. and A.H. Guenther, *Laser-Induced Damage Of Optical Elements - Status Report.* Applied Optics, 1973. **12**(4): p. 637-649.
5. Demos, S.G., M. Staggs, and M.R. Kozlowski, *Investigation of processes leading to damage growth in optical materials for large-aperture lasers.* Applied Optics, 2002. **41**(18): p. 3628-3633.
6. Bude, J., et al., *The effect of lattice temperature on surface damage in fused silica optics - art. no. 672009.* Laser-Induced Damage in Optical Materials: 2007, 2008. **6720**: p. 672009.
7. Jones, S.C., et al., *Recent progress on laser-induced modifications and intrinsic bulk damage of wide-gap optical materials.* Optical Engineering, 1989. **28**(10): p. 1039-.
8. Papernov, S. and A.W. Schmid, *Correlations between embedded single gold nanoparticles in SiO2 thin film and nanoscale crater formation induced by pulsed-laser radiation.* Journal of Applied Physics, 2002. **92**(10): p. 5720-5728.
9. Norton, M.A., et al., *Growth of laser initiated damage in fused silica at 527 nm.* Laser-Induced Damage In Optical Materials: 2003, 2003. **5273**: p. 236-243.
10. Laurence, T.A., et al., *Metallic-like photoluminescence and absorption in fused silica surface flaws.* Applied Physics Letters, 2009. **94**(15): p. 151114.
11. Pacchioni, G., L. Skuja, and D.L. Griscom, *Defects in SiO_2 and related dielectrics: science and technology*. NATO science series. Series II, Mathematics, physics, and chemistry; v. 2. 2000, Dordrecht, Netherlands, Boston, MA: Kluwer Academic Publishers. viii, 624 p.
12. Skuja, L., *The Origin of the Intrinsic 1.9 Ev Luminescence Band in Glassy Sio2.* Journal of Non-Crystalline Solids, 1994. **179**: p. 51-69.
13. Skuja, L., *Optically active oxygen-deficiency-related centers in amorphous silicon dioxide.* Journal of Non-Crystalline Solids, 1998. **239**(1-3): p. 16-48.
14. Beversluis, M.R., A. Bouhelier, and L. Novotny, *Continuum generation from single gold nanostructures through near-field mediated intraband transitions.* Physical Review B, 2003. **68**(11): p. 115433.
15. Boyd, G.T., Z.H. Yu, and Y.R. Shen, *Photoinduced luminescence from the noble metals and its enhancement on roughened surfaces.* Physical Review B, 1986. **33**(12): p. 7923.
16. Mooradian, A., *Photoluminescence of Metals.* Physical Review Letters, 1969. **22**(5): p. 185.
17. Demos, S.G., Y. Takiguchi, and R.R. Alfano, *Up-Converted Hot-Luminescence Spectroscopy Investigation Of Nonradiative Relaxation In Forsterite.* Optics Letters, 1993. **18**(7): p. 522-524.
18. Hibino, Y. and H. Hanafusa, *Stress-Induced Photoluminescence in Pure Silica Optical Fibers.* Journal of Non-Crystalline Solids, 1988. **107**(1): p. 23-26.
19. Kucheyev, S.O. and S.G. Demos, *Optical defects produced in fused silica during laser-induced breakdown.* Applied Physics Letters, 2003. **82**(19): p. 3230-3232.
20. Sun, H.B., et al., *Generation and recombination of defects in vitreous silica induced by irradiation with a near-infrared femtosecond laser.* Journal of Physical Chemistry B, 2000. **104**(15): p. 3450-3455.
21. Stevens-Kalceff, M.A. and J. Wong, *Distribution of defects induced in fused silica by ultraviolet laser pulses before and after treatment with a CO[sub 2] laser.* Journal of Applied Physics, 2005. **97**(11): p. 113519.
22. Anedda, A., et al., *Visible and ultraviolet emission of porous silica excited by synchrotron radiation.* Journal of Non-Crystalline Solids, 2005. **351**(21-23): p. 1924.
23. Hagan, J.T., *Cone Cracks Around Vickers Indentations In Fused Silica Glass.* Journal Of Materials Science, 1979. **14**(2): p. 462-466.